Journal of Crystal Growth 125 (1992) 389–403
North-Holland

JOURNAL OF CRYSTAL GROWTH

A numerical study of the combined effect of anisotropic surface tension and interface kinetics on pattern formation during the growth of two-dimensional crystals

Etsuro Yokoyama [1] and Robert F. Sekerka

Departments of Physics and Mathematics, Carnegie Mellon University, Pittsburgh, Pennsylvania 15213-3890, USA

Received 27 December 1991; manuscript received in final form 5 August 1992

We study the combined effect of anisotropic surface tension and interface kinetics on pattern formation during the growth of two-dimensional crystals under conditions such that the growth is governed by interfacial processes. For sinusoidal anisotropies having fourfold symmetry, we compute numerically the trajectories of elements of the interface having constant crystallographic orientation. Our results display many of the features derived from general consideration by Angenent and Gurtin. We concentrate on the formation or suppression of corners (missing orientations) and develop an asymptotic analytical representation to explain our results. As a test of our numerical techniques, we treat the very special case for which the anisotropy of surface tension is proportional to the anisotropy of the interface kinetic coefficient, and show that the growth pattern, starting from a shape similar to the equilibrium shape, preserves its shape, as proven by Soner.

1. Introduction

The formation of patterns in crystal growth is a free-boundary problem in which the interface that separates the crystal from a nutrient phase moves under the influence of nonequilibrium conditions [1–5]. The resulting patterns depend markedly on conditions in the nutrient phase, e.g. temperature and concentration, which influence the growth speed of each element of the interface. Furthermore, the growth speed of each element also depends on the local geometry of the interface, specifically on the interface curvature and the orientation of the interface relative to the crystal axes.

The local growth speed of an interface can, in principle, be determined by solving the transport equations that take into account the following elementary processes: (1) a diffusion process for the transport of latent heat and/or solute liberated at the interface, and (2) an interface kinetic process [6–9] for transformation of an amorphous phase into a crystalline phase at the interface at a rate determined by the deviation from local equilibrium conditions, which depend on interface curvature.

The combined effect of anisotropic kinetics and surface tension on crystal growth has been treated in a few special cases, e.g. with respect to the morphological instability of spheres [10], circular cylinders [11] and planes [12]. The stabilizing influence of kinetics and surface tension on large facets has been discussed [13]. Moreover, the possible effect of anisotropy on the growth of the primary stalk of a dendrite has been investigated [14–18]. It has been shown that anisotropic surface tension plays an important role in stabilizing the tip of a dendrite primary stalk in the absence of interface kinetics [16–17]. A study of the effect of anisotropy of interface kinetics on crystal growth forms has been carried out [18], in which it was found that the anisotropic interface

[1] Present address: Faculty of Computer Science and Systems Engineering, Kyushu Institute of Technology, Iizuka 820, Japan.

kinetics can also act to suppress tip splitting. Severe anisotropy of interface kinetics, for which the kinetic coefficient has singularities in the form of deep cusps, plays a very important part in the formation of facted shapes in growth from a vapor, such as for snow crystals [19].

Cahn, Taylor and Handwerker [20] have published an extensive review of the classical work of Frank [21] on the motion of boundaries governed by a local anisotropic kinetic law and have extended this work in several aspects. More recently, Taylor, Cahn and Handwerker [22] have set forth nine methodologies for solving such problems. Taylor [23] has also investigated the fundamental mathematical basis of boundaries that move according to a law that depends on mean curvature or weighted mean curvature.

Gurtin [24] has derived equations and boundary conditions for boundary evolution under the influence of anisotropic kinetics and surface tension from very general principles: force balance, energy balance, and entropy production. His boundary conditions are of a similar form to those used previously [10–12]. Such boundary conditions were motivated previously on the basis that the growth speed must be the same whether calculated from balance laws or from irreversible kinetic processes on an atomistic scale that depend on conditions local to the interface. Subsequently, Angenent and Gurtin [25] have made an extensive analytical study of boundary motion in two dimensions for an isothermal interface moving under the influence of anisotropic surface tension and kinetics. Our results for a specific choice of anisotropy display many of the features derived from general considerations by Angenent and Gurtin.

In this article, we examine the combined effect of anisotropic surface tension and interface kinetics on pattern formation during the growth of a two-dimensional crystal under conditions such that the transport of heat and/or solute is so rapid that growth is controlled by interfacial processes. In particular, we study by numerical methods the influence of sinusoidal anisotropies having fourfold symmetry on the formation or suppression of corners of a crystal, starting from a crystal of circular shape. As a test case of our numerical methods, we also treat the very special case in which the kinetic coefficient and the surface tension are proportional, starting from a shape similar to the equilibrium shape.

Numerical models for time evolution of an interface have recently been developed [16–19,26]. They are, however, unsatisfactory for the description of trajectories of elements of interface having constant crystalline orientation. To compute these trajectories and the concomitant interface shape, we perform a direct numerical integration of a nonlinear equation for the interface curvature. For the case in which the growth speed is independent of curvature, these trajectories are characteristic curves of the underlying differential equation [20–22,27,28].

The layout of this paper is as follows. In section 2, our model and equations for tracking an interface are introduced. In section 3, we present the numerical results of time evolution of an interface. Finally, in section 4, we discuss these results.

2. The model

2.1. Growth speed of the interface

We begin by considering a two-dimensional one-sided model (transport only in the liquid phase) in which an undercooled liquid phase surrounds a single crystal of pure material, and proceed to show how this leads to a local model when transport in the bulk phase is very rapid.

We rescale all lengths by an amount

$$R^* = \frac{\gamma_0 T_M}{L(T_M - T_\infty)}, \tag{1}$$

where γ_0 is the average surface tension, L is the latent heat of fusion per unit volume of the crystal, T_M is the bulk melting temperature of a pure material and T_∞ is the liquid temperature far from the interface. For isotropic surface tension, R^* would be the nucleation radius. Time is scaled by

$$t^* = \frac{(R^*)^2}{\alpha} \frac{L/c_L}{T_M - T_\infty}, \tag{2}$$

where α is the thermal diffusivity and c_L is the specific heat per unit volume of the liquid.

Assuming that the interface moves sufficiently slowly that the thermal field has time to relax practically to its steady state value, the temperature field is governed by the Laplace equation,

$$\Delta U = 0, \tag{3}$$

where U is the dimensionless temperature given by $U = (T - T_\infty)/(T_M - T_\infty)$. The boundary conditions are as follows:

$$U(R_\infty) = 0, \tag{4}$$

$$-(\nabla U \cdot \hat{\boldsymbol{n}})_{\text{interface}} = V, \tag{5}$$

where R_∞ is the dimensionless radius of the outer boundary, $\hat{\boldsymbol{n}}$ is the unit normal vector to the solid–liquid interface, pointing into the liquid, and V is the local normal growth speed of the interface.

If we define the thickness, δ, of the dimensionless thermal diffusion boundary layer by the equation $U_I/\delta = (-\nabla U \cdot \hat{\boldsymbol{n}})_{\text{interface}}$, where U_I is the interfacial temperature, we can rewrite eq. (5) in the form

$$U_I/\delta = V. \tag{6}$$

We assume that the local normal growth speed, V, of the interface is also calculable from irreversible interface kinetic processes on an atomistic scale that depend on conditions local to the interface, resulting in an equation of the form

$$V = \beta(\theta)\ (U_E - U_I), \tag{7}$$

where $\beta(\theta)$ is the dimensionless kinetic coefficient scaled by R^*/t^*, θ is the angle made by the normal to the interface and a principal crystal axis, and U_E is the local equilibrium melting temperature. The quantity U_E depends on the dimensionless local curvature K, the surface tension γ, scaled by the average surface tension γ_0, and the second derivative of γ with respect to θ, according to the equation

$$U_E = 1 - (\gamma + \gamma_{\theta\theta})K. \tag{8}$$

In eq. (7), $\beta(\theta)$ represents the relative rate of growth of the crystalline phase into the liquid phase. We assume that β depends only on θ; whereas, more generally, β depends also on other factors such as U_I and K [12].

Substituting U_I of eqs. (6) and (8) into eq. (7), we obtain the self-consistent growth speed:

$$V = \frac{1 - (\gamma + \gamma_{\theta\theta})K}{\beta^{-1} + \delta}. \tag{9}$$

The denominator of eq. (9) represents the relative resistances of each process [30–32]. In general, δ is a function of position along the interface, and must be determined by solution of a nonlocal problem. Assuming, however, that the transport of heat is rapid, we can neglect δ compared to β^{-1}, and the growth speed V is determined by local kinetic processes. Thus, approximately,

$$V \simeq \beta(\theta)\ [1 - (\gamma + \gamma_{\theta\theta})K]. \tag{10}$$

The remainder of this paper is based on the supposition that eq. (10) is exact. It has the same form as eq. (1.2) of Angenent and Gurtin [25].

2.2. Equations of the growing interface

Fig. 1 shows schematically part of a growing interface. Let $\boldsymbol{r}(u, t)$ represent the position vector of the interface at a given time t, where u is a

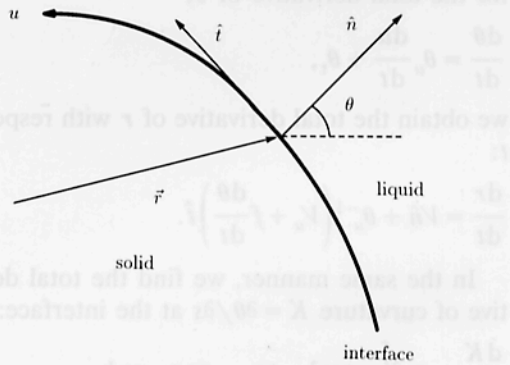

Fig. 1. Schematic illustration of a growing interface between solid (crystal) and liquid. At position $\boldsymbol{r}$, $\hat{\boldsymbol{n}}$ is the local normal vector that makes an angle θ with respect to the x axis and $\hat{\boldsymbol{t}}$ is the local tangent vector in the direction of increasing values of the parameter u.

suitably chosen parameter. In Cartesian coordinates,

$$\boldsymbol{r} = (x(u, t), y(u, t)). \tag{11}$$

The partial derivative of $\boldsymbol{r}$ with respect to t holding u constant is

$$\boldsymbol{r}_t = V\hat{\boldsymbol{n}} + V_\perp \hat{\boldsymbol{t}}, \tag{12}$$

in which $V_\perp$ is a tangential growth speed of the interface for growth along trajectories of constant u, $\hat{\boldsymbol{n}}$ is the unit outward normal vector and $\hat{\boldsymbol{t}}$ is the unit tangent vector pointing toward increasing u. The unit vectors $\hat{\boldsymbol{n}}$ and $\hat{\boldsymbol{t}}$ are given by

$$\hat{\boldsymbol{n}} = (\cos\theta, \sin\theta), \quad \hat{\boldsymbol{t}} = (-\sin\theta, \cos\theta), \tag{13}$$

where $\cos\theta = y_u/(x_u^2 + y_u^2)^{1/2}$ and $\sin\theta = -x_u/(x_u^2 + y_u^2)^{1/2}$, in which subscripts denote partial differentiation.

The partial derivative of $\boldsymbol{r}$ with respect to u holding t constant is

$$\boldsymbol{r}_u = f(u, t)\hat{\boldsymbol{t}}, \tag{14}$$

in which $f(u, t) = |\boldsymbol{r}_u|$, that is, $f = \partial s/\partial u$. Here s is arc length of the interface, measured positively in the direction of increasing u.

We differentiate eq. (12) by u and eq. (14) by t. Assuming conditions such that the order of differentiation is irrelevant, we obtain

$$-f\theta_t = V_u - \theta_u V_\perp, \tag{15}$$

$$f_t = V\theta_u + \partial V_\perp/\partial u. \tag{16}$$

From eqs. (12), (14) and (15), and the equation for the total derivative of θ,

$$\frac{\mathrm{d}\theta}{\mathrm{d}t} = \theta_u \frac{\mathrm{d}u}{\mathrm{d}t} + \theta_t, \tag{17}$$

we obtain the total derivative of $\boldsymbol{r}$ with respect to t:

$$\frac{\mathrm{d}\boldsymbol{r}}{\mathrm{d}t} = V\hat{\boldsymbol{n}} + \theta_u^{-1}\left(V_u + f\frac{\mathrm{d}\theta}{\mathrm{d}t}\right)\hat{\boldsymbol{t}}. \tag{18}$$

In the same manner, we find the total derivative of curvature $K = \partial\theta/\partial s$ at the interface:

$$\frac{\mathrm{d}K}{\mathrm{d}t} = f^{-2}\left[-V\theta_u^2 - V_{uu} + V_u\theta_{uu}\theta_u^{-1} + \left(-f_u + f\theta_{uu}\theta_u^{-1}\right)\frac{\mathrm{d}\theta}{\mathrm{d}t}\right]. \tag{19}$$

We treat the case of a convex crystal, in which case $\boldsymbol{r}(\theta, t)$ is a single valued function of θ. We choose $u = \theta$ in which case $f = \partial s/\partial\theta = K^{-1}$. Then, we examine trajectories of constant θ, in which case $\mathrm{d}\theta/\mathrm{d}t = 0$, and eqs. (18) and (19) take the form

$$\left(\frac{\mathrm{d}\boldsymbol{r}}{\mathrm{d}t}\right)_{\text{along } \theta = \text{const.}} = V\hat{\boldsymbol{n}} + \frac{\partial V}{\partial\theta}\hat{\boldsymbol{t}}, \tag{20}$$

$$\left(\frac{\mathrm{d}K}{\mathrm{d}t}\right)_{\text{along } \theta = \text{const.}} = -K^2\left(V + \frac{\partial^2 V}{\partial\theta^2}\right), \tag{21}$$

where t is held constant in the derivatives with respect to θ.

Under the condition that V depends only on θ, the ratio V to $\partial V/\partial\theta$ in eq. (20) is a constant for a given θ, and the trajectories are straight lines, as is well known [21]. For V given by eq. (10), eq. (21) becomes

$$K_t = K^2\left[(\alpha K)_{\theta\theta} + \alpha K - (\beta_{\theta\theta} + \beta)\right], \tag{22}$$

where $\alpha = \beta(\gamma + \gamma_{\theta\theta})$. Eq. (22) is the same (except for notation and sign convention) as eq. (5.6) of Angenent and Gurtin [25]. Provided that $\alpha > 0$, this equation is just a nonlinear diffusion equation for K and can be integrated numerically.

In the next section, we show the results of numerical integration of eq. (22) for sinusoidal anisotropies having fourfold symmetry, along with the corresponding interface shapes. We do not treat the case of $\alpha < 0$ for which eq. (22) is backward parabolic and has been discussed by Angenent and Gurtin.

3. Numerical results

We assume that the anisotropy of the kinetic coefficient is sinusoidal and has fourfold symmetry as follows:

$$\beta(\theta) = \beta_0\left[1 - \epsilon_1\cos(4\theta)\right], \tag{23}$$

where β_0 is a constant, θ is the angle between $\hat{\boldsymbol{n}}$ and the x axis, and ϵ_1 characterizes the degree of anisotropy.

Fig. 2 shows the growth pattern for anisotropic interface kinetics for $\beta_0 = 0.1$ and $\epsilon_1 = 0.2$ in the

absence of surface tension ($\gamma(\theta) = 0$) for an initial crystal radius $R_0 = 2$. The trajectories shown in the first quadrant are straight lines, and the crystal develops sharp corners (places where there are missing orientations) that sharpen with time as the crystal approaches an asymptotic shape.

We next consider the effect of surface tension on crystal shape. We assume a form of anisotropy of surface tension similar to the anisotropy of the kinetic coefficient:

$$\gamma(\theta) = 1 - \epsilon_2 \cos(4\theta). \tag{24}$$

Here, ϵ_2 gives the degree of anisotropy. Fig. 3a shows the growth pattern for the same conditions as fig. 2 except for isotropic surface tension, i.e. $\epsilon_2 = 0$, so that $\gamma(\theta) = 1$. Fig. 3b shows the curvature as a function of θ for each time step corresponding to fig 3a. Fig. 3c shows the curvature for some early times when the deviations from constant curvature are developing. Thus the curvature first deviates from its initially constant value of 0.5, forming a peak near $\theta = \pi/4$ which decays with time as illustrated in fig. 3b. Sharp corners on the growth pattern do not develop because of the Gibbs-Thomson effect which dominates for large K. We note that the trajectories near these rounded corners tend toward parallel lines instead of converging along shocks to produce sharp corners, as in fig. 2.

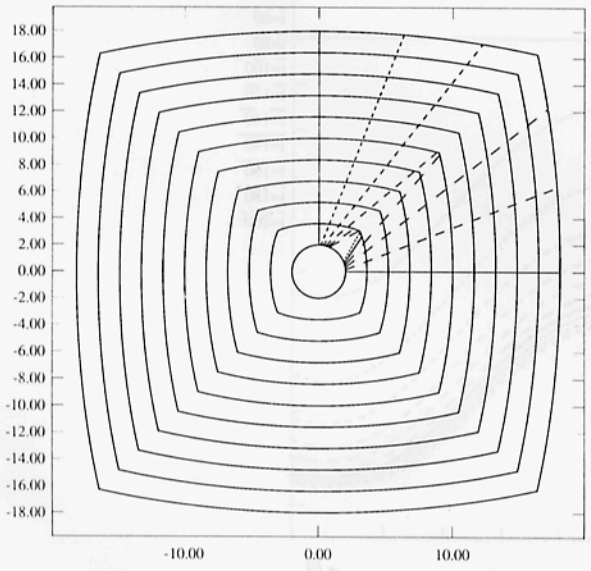

Fig. 2. Growth pattern for anisotropic interface kinetics in the absence of surface tension, i.e. $\gamma(\theta) = 0$. The contours represent the interface at equal intervals ($\Delta t = 20$) of time beginning with $t = 0$. The anisotropy of the kinetic coefficient is given by eq. (23) with $\beta_0 = 0.1$ and $\epsilon_1 = 0.2$. The initial crystal radius $R_0 = 2$.

The growth pattern for the same conditions as fig. 3 except for isotropic kinetics, i.e. $\epsilon_1 = 0$, is shown in fig. 4a. Fig. 4b shows the curvature as a function of θ for each time step corresponding to fig 4a. Deviations from circularity are evident at short times because of the anisotropic surface tension which affects the growth pattern for crystals of small size and large K. The patterns become more rounded with increasing crystal size because of the decrease of K, and the peak of curvature fades away with time as shown in fig. 4b.

The combined effect of anisotropic surface tension, $\epsilon_2 = 0.05$, and anisotropic interface kinetics, $\epsilon_1 = 0.2$, on crystal pattern is shown in fig. 5a. The corresponding curvature as a function of θ for each time step is shown in fig. 5b. The major change, in comparison with fig. 3, is that the corners have higher curvature, and a strong peak in the curvature remains, as shown in fig. 5b. This occurs because ϵ_1 and ϵ_2 have been chosen to have the same sign. We discuss the asymptotic form of these rounded corners in detail in the next section.

Soner [29] has shown that if the anisotropy of the surface tension is proportional to the anisotropy of the interface kinetic coefficient, i.e. $\epsilon_1 = \epsilon_2$ in our case, and the initial shape is chosen to be geometrically similar to the equilibrium shape, then the growth pattern preserves its shape for all time. For $\epsilon_2 < 1/15$, we have $\gamma + \gamma_{\theta\theta} > 0$, and the equilibrium shape corresponding to $V = 0$ in eq. (10) is given by [33]

$$\boldsymbol{r}_{\mathrm{eq}}(\theta) = \gamma \hat{\boldsymbol{n}} + \gamma_\theta \hat{\boldsymbol{t}}. \tag{25}$$

In fig. 6 we demonstrate numerically that the growth pattern, starting from a shape similar to but five times larger than that given by eq. (25), preserves its shape for $\epsilon_1 = \epsilon_2 = 0.03$. This provides a test of our numerical methods. In the next

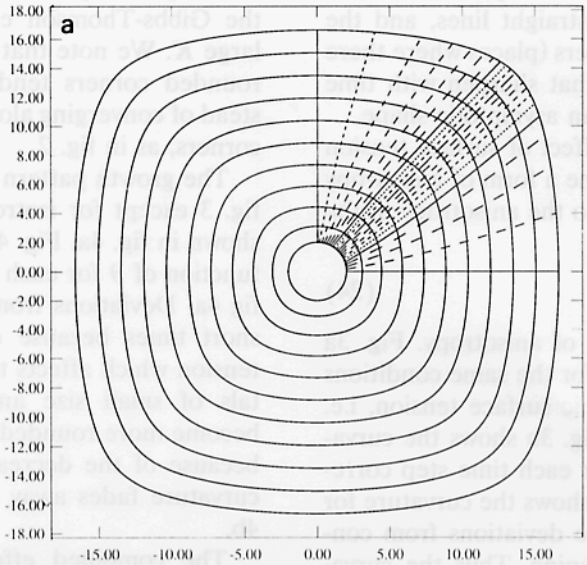

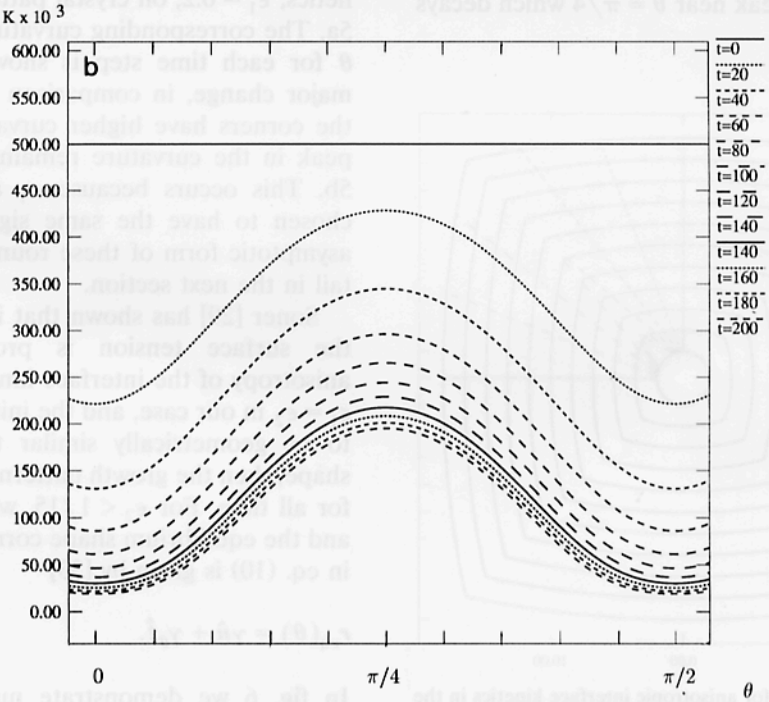

Fig. 3. (a) Growth pattern for anisotropic interface kinetics in the presence of isotropic surface tension, i.e. $\gamma(\theta) = 1$. The anisotropy of the kinetic coefficient is given by eq. (23) with $\beta_0 = 0.1$ and $\epsilon_1 = 0.2$. The initial crystal radius $R_0 = 2$. The time intervals are the same as for fig. 2. (b) The curvature as a function of θ for each time step corresponding to (a). (c) The curvature corresponding to (a) as a function of θ from $t = 0$ to $t = 2$. The deviations from constant curvature $K = 0.5$ are developing with time. The time intervals are $\Delta t = 0.2$.

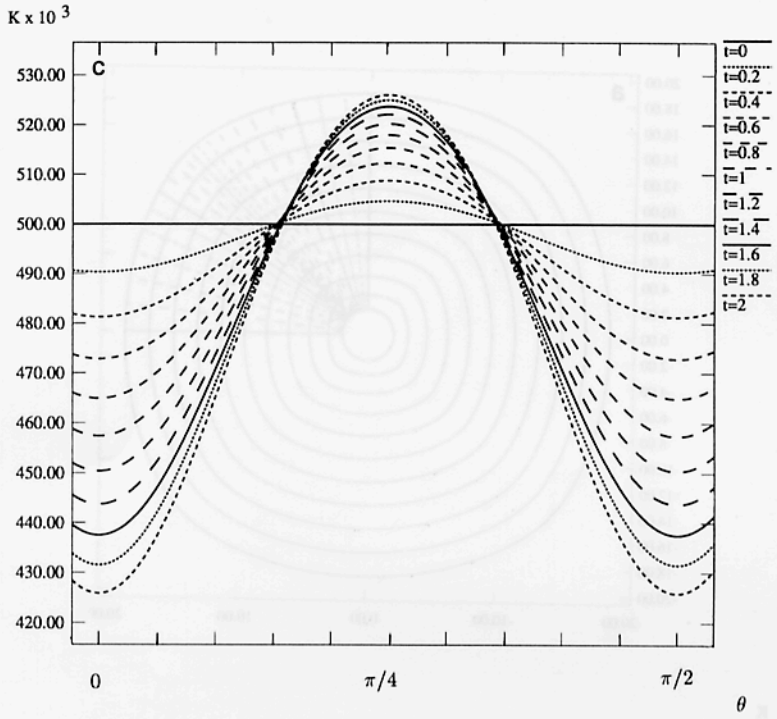

Fig. 3. Continued.

section, we discuss further why the growth form preserves its shape under these conditions.

4. Discussion

We first discuss the asymptotic shape of corners. Frank [21] proved that the trajectory of an element having constant orientation on the interface is parallel to the normal to the polar diagram of the reciprocal, V^{-1}, of the growth speed at this orientation. We show in fig. 7 the polar diagram of $(V/\beta_0)^{-1}$ corresponding to fig. 2; here, V^{-1} depends on the orientation θ. From Frank's theory, the following results may be deduced [34]: The normals to the polar diagram between the tangent points P_1 and P_2 in fig. 7 are converging. As a result, the trajectories in fig. 2 corresponding to the orientations between P_1 and P_2 will intersect and disappear, and the asymptotic shape will not have orientations between P_1 and P_2. Starting from a circle, corners form and sharpen with time as more orientations between P_1 and P_2 become missing, resulting asymptotically in corners determined by the orientations corresponding to P_1 and P_2.

On the other hand, if the growth speed V depends not only on θ but also on the curvature K, the polar diagram of V^{-1} changes, because K changes with time. Fig. 8 shows polar diagrams of $(V/\beta_0)^{-1}$ corresponding to fig. 3a at two different times; the solid line corresponds to the initial shape in fig. 3a and the dotted line corresponds to the final shape in fig 3a. The dotted line is convex and is nearly straight near the $\pi/4$ direction, as well as in other directions related by symmetry; the corresponding trajectories of constant orientation in fig. 3a are parallel lines near these directions and the rounded corners have nearly constant curvature.

We next consider the asymptotic shape of the rounded corners in figs. 3, 4 and 5 as a function of the anisotropies of $\beta(\theta)$ and $\gamma(\theta)$. We conjecture that an asymptotic shape exists near these